Ambi-site substitution of Mn in lanthanum germanate apatites

Kendrick, Emma; Knight, K. S.; Slater, Peter

DOI:
10.1016/j.materresbull.2009.03.002

Document Version
Peer reviewed version

Citation for published version (Harvard):
Kendrick, E, Knight, KS & Slater, P 2009, 'Ambi-site substitution of Mn in lanthanum germanate apatites', *Materials Research Bulletin*, vol. 44, no. 8, pp. 1806-1809. https://doi.org/10.1016/j.materresbull.2009.03.002

Ambi-site substitution of Mn in Lanthanum Germanate Apatites

E. Kendrick[1], K.S. Knight[2], P.R. Slater[3*]

[1]Chemical Sciences, University of Surrey, Guildford, Surrey. GU2 7XH. UK

[2] ISIS Facility, Rutherford Appleton Laboratory, Harwell Science and Innovation Campus, Didcot, OX11 0QX. UK

[3] School of Chemistry, University of Birmingham, Birmingham B15 2TT. UK

[*]Correspondence to:

Dr. P.R. Slater

School of Chemistry, University of Birmingham, Birmingham B15 2TT. UK

Tel. +44 (0)121 4148906

Fax +44 (0)121 4144403

p.r.slater@bham.ac.uk

Abstract

A neutron diffraction study at 4K of the Mn doped lanthanum germanate apatite-type oxide ion conductor of nominal starting composition "$La_{9.5}Mn_{0.5}(GeO_4)_6O_{2.75}$" is reported. The structure was refined in space group $P6_3/m$, although high thermal displacement parameters were observed for the oxide ion sites (particularly O3, and O4). Reduced thermal displacement parameters were obtained by splitting the O3 site, and allowing the O4 oxygen to move off site, which may indicate local regions of lower symmetry within the structure. In addition, the data suggested ambi-site substitution of Mn, with it being present on both the Ge site and the La site. Assuming no change in La:Mn:Ge ratio, a composition of $La_{9.18}Mn_{0.28}(GeO_4)_{5.8}(MnO_4)_{0.2}O_2$ was determined. As such there are nominally no interstitial oxide ions, but rather cation vacancies on the La site. Therefore, the high conductivity for this sample is most likely related to the introduction of Frenkel-type defects at higher temperature, as previously proposed for other apatite-type systems containing vacancies on the La site

Keywords: A. Oxides, B. Chemical Synthesis, C. Neutron scattering, D. Ionic conductivity

Introduction

Interest in apatite silicates/germanates, $Ln_{9.33+x}(Si/GeO_4)_6O_{2+3x/2}$ (Ln=rare earth) has grown in recent years, following numerous reports of high oxide ion conduction in these materials, giving potential applications as solid oxide fuel cell electrolytes [1-36]. An important aspect of these apatite materials is that oxide ion conduction is mediated by interstitial oxide ions, in contrast to the traditional fluorite and perovskite oxide ion conductors, where a vacancy mechanism is dominant [5,7,8]. As a result, it has been shown that fully stoichiometric, e.g. $La_8Sr_2(Si/GeO_4)_6O_2$, samples show poor conductivity, while samples containing oxygen excess, e.g. $La_9Sr(Si/GeO_4)_6O_{2.5}$, or cation vacancies, e.g. $La_{9.33}(Si/GeO_4)_6O_2$ show high conductivity. For the latter systems, it has been proposed that the cation vacancies cause local structural distortions, which promote Frenkel-type disorder [5]. The crystal structure of these apatite systems in shown in figure 1; they may be classed in two ways, either in terms of an $La_{3.33+x}(Si/GeO_4)_6$ framework, with the remaining La_6O_2 units accommodated in the "cavities" within the framework [17]. Alternatively they may be described as comprising of isolated Si/GeO_4 tetrahedra arranged so as to form distinct oxide ion and La channels running parallel to the *c* axis. With regard to the interstitial oxide ions, computer modelling studies have predicted that the most favourable interstitial oxide ion site is at the periphery of the oxide ion channels neighbouring the SiO_4/GeO_4 groups, and highlighted the important role played by relaxation of the SiO_4/GeO_4 substructure in the high oxide ion conductivity [8,23,27]. The

conclusions of this modelling work have been supported by structural studies of oxygen excess systems, $La_{9.33+x}(Si/GeO_4)_6O_{2+3x/2}$ [7,12,13,19,26,34].

Much of the work on doping apatite systems has focused on the silicate systems, due to problems with Ge volatility at temperatures above 1400 °C in the germanates, with such high temperatures being required to obtain sintered pellets. As a result of this sintering problem, we have investigated means of lowering the sintering temperature through doping studies. In this respect, we have shown that doping transition metals (Co, Mn) on the La site, according to the nominal formula, $La_{10-x}M_y(GeO_4)_6O_{2+z}$ (M=Mn, Co) leads to samples with high conductivity (0.01-0.02 Scm^{-1} at 800 °C) that can be sintered to high density at 1300-1400 °C [37]. In this paper, we report the crystal structure of such a Mn doped sample, with nominal composition, "$La_{9.5}Mn_{0.5}(GeO_4)_6O_{2.75}$", using neutron diffraction. Since these apatite-type oxide ion conductors tend to show high thermal displacement parameters associated with static disorder [22], data were collected at low temperature (4.2 K) in order to reduce these thermal displacement parameters, and hence gain more accurate information on the oxide ion sites.

Experimental

A 5 g sample of nominal composition, "$La_{9.5}Mn_{0.5}(GeO_4)_6O_{2.75}$", was prepared from high purity La_2O_3, GeO_2, MnO_2 which were intimately mixed in the correct molar ratios and heated to 1100 °C for 14 hours, reground and then reheated to 1200 °C for a further 14 hours. Phase purity was established through X-ray powder diffraction (Panalytical X'Pert Pro diffractometer, Cu $K\alpha_1$ radiation).

Neutron diffraction data were collected on the diffractometer HRPD at the ISIS spallation source, Rutherford Appleton Laboratory, UK. The sample was loaded into a thin-walled cylindrical vanadium can, which was then placed in a cryostat, with the data collected at 4.2 K. Structure refinement was performed using the GSAS suite of Rietveld refinement software [38]. Data sets from two banks of detectors were used for the refinement; the first was the data from the backscattering detector bank and the second was the data from the 90° detector bank.

Results and discussion

Space group $P6_3/m$, which is typical for apatite systems, was employed, with an initial model consisting of full occupancy of the oxygen sites, and no interstitial oxide ions. The Mn and cation vacancies were initially located on the La1 site, in agreement with prior experimental and modelling work, supporting the preference of lower valent cations and vacancies for this site [22]. This gave a reasonably good fit to the data (χ^2= 4.67). Introduction of Mn on the La2 site gave a significantly worse fit (χ^2= 5.66), confirming the assignment of the Mn on the La1 site. With this good basic starting model, Difference Fourier maps were plotted in an attempt to locate any interstitial oxide ion sites. These Fourier maps showed a negative nuclear density very close to the Ge position. Considering the neutron scattering lengths of Ge and Mn (8.185 fm and -3.73 fm respectively), this suggested the presence of some Mn on the Ge site. Refinement of the relative site occupancies suggested values of 0.967(3) and 0.033(3) for Ge and Mn respectively. With the presence of some Mn on the Ge site, the Mn occupancy on the La site must be comparatively reduced. The freely refined La site occupancy of the La1 site

assuming only La present was found to be 0.742(7). Due to the presence of three variables (La, Mn, and cation vacancies) for this site, it was not possible to refine individual La and Mn occupancies. However, considering the refined Ge/Mn occupancies on the "Ge" site, and assuming no change in La:Ge:Mn ratio, the expected occupancy of the "La1" site was determined as 0.795 La, 0.07 Mn, 0.135 cation vacancies. Assuming these occupancies, an expected overall "La1" site occupancy value of 0.760 is obtained, which is close to the observed value of 0.742(7). Therefore this predicted La site occupancy was used, and hence the cation distribution was fixed as $(La_{9.18}Mn_{0.28})(Ge_{5.8}Mn_{0.2})$ in the final refinement. With this cation distribution, the expected oxygen content was then determined. Assuming Mn substitutes on the La site as Mn^{2+}, and on the Ge site as Mn^{3+}, as predicted by modelling studies [24], and observed experimentally for related Mn and Co doped silicate apatites [20, 39, 40], an oxygen content of 26.0 would be obtained, suggesting no interstitial oxide ions present. In order to confirm this, a close inspection of the Fourier maps was performed. This showed a large spread of nuclear density along z for the O4 site, consistent with the very high thermal displacement parameters observed for this site ($100 \times U_{33}=17$ Å^2). Considering that the data was collected at 4.2 K, this spread of nuclear density cannot be due to thermal motion and is indicative of static disorder. Therefore the O4 oxide ion was allowed to move off site along z to give a split site, which resulted in a significant reduction in the thermal displacement parameter. Apart from the O4 site, the O3 site showed a similarly high thermal displacement parameter ($100 \times U_{22}= 12$ Å^2), with Fourier maps again suggesting the need for a split site. Therefore two sites 03a and 03b were introduced, and the occupancies of each refined such that the total occupancy was

1.0. This led to refined site occupancies of 0.26 and 0.74, a reduced thermal displacement parameter, and an improved fit. As far as the presence of interstitial oxide ion sites was concerned, there was an indication of a small amount of unfitted nuclear density at (0.363, 0.401, 0.25), but the refined occupancy was zero within errors (0.004(4)), and hence this site was not included in the final refinement. The lack of interstitial oxide ions is consistent with the refined cation composition described earlier. The final refined parameters are shown in table 1 with selected bond distances in table 2, and neutron diffraction profiles shown in figure 2.

The data shows that Mn is an ambi-site dopant, substituting on both the La and Ge sites. While Mn substitution on the large cation and tetrahedral sites have both previously been reported [39-42], the data here shows the first example of partitioning over both sites in the same sample. The driving force for Mn to substitute onto the Ge site is most likely due to the reduction in the interstitial oxide ion content (expected interstitial oxide ion content = 0.75 assuming Mn only on the La site and no cation vacancies, compared with the refined occupancy of zero, with Mn on both the La and Ge site and the presence of cation vacancies) showing that the presence of cation vacancies is more favourable than interstitial oxide ions in this system. Considering the lack of interstitial oxide content in this sample, and the known importance of interstitial oxide ions in the conduction mechanism of apatite-type oxide ion conductors, it was decided to investigate the conductivity of the sample used in the neutron diffraction experiment to compare with the previous observation of high conductivity in similar Mn doped samples [37]. Pellets (1.3 cm diameter) for conductivity measurements were prepared as follows: the powders were ball milled (350 rpm, Fritsch Pulverisette 7 Planetary Mill) for 2 hours before pressing at

8000 kg cm^{-2}. The pressed pellets were then heated at 1350 °C for 2 hours, leading to a density of 88 % theoretical. Both sides of the pellet were coated with Au paste and then heated to 700 °C for 1 hour to ensure bonding to the pellet. Conductivity measurements were made in air using a Solarton 1287 impedance analyzer. Measurements were made in both oxygen and nitrogen to determine whether there was any significant electronic contribution to the conductivity. No significant difference was observed, consistent with the conductivity being dominated by the oxide ion contribution. The conductivity data is shown in figure 3, which shows that despite the low interstitial oxide ion content, the conductivity is high (0.012 Scm^{-1} at 800 $^{\circ}C$), in agreement with our prior work on a sample with a similar nominal starting composition (0.016 Scm^{-1}) [37]. This high conductivity, is most likely due to the introduction of Frenkel-type disorder at higher temperatures, as proposed previously for apatite systems containing cation vacancies [22].

Another interesting result from the refinement is the large thermal displacement parameters for the oxide ion sites, especially O3 and O4 sites. As noted earlier, the fact that the data was collected at low temperature (4.2 K) means that these large displacements are correlated with static displacements rather than thermal motion. Reduced thermal displacement parameters were therefore obtained by splitting the O3 site and allowing the O4 ion to move off site. It is interesting to comment on the origin of these displacements/split sites. The O3 sites in space group $P6_3/m$ lie either side of the mirror plane, and loss of this mirror plane (lower symmetry space group $P6_3$), leads to the O3 site being split into two sites. Similarly in space group $P6_3/m$ the O4 site has ideal position (0, 0, ¼), whereas lowering the symmetry to $P6_3$ allows for displacement along

z. The observed split sites might therefore be an indication of a lowering in symmetry to $P6_3$. However, this might have been expected to lead to occupancies of 0.5 each for O3a and O3b, whereas the actual values were 0.74 and 0.26. Similarly attempts at refinement in space group $P6_3$ still resulted in high thermal displacement parameters for the O4 channel site, whereas with the split site in space group $P6_3/m$, a lower parameter was obtained, consistent with the average space group being $P6_3/m$. The results may, however, indicate that whereas the average structure has space group $P6_3/m$, locally there are regions of lower ($P6_3$, or monoclinic, triclinic) symmetry, which is probably a general feature of these apatite systems, and hence would explain the high thermal displacement parameters observed in this work and other structural studies in the literature.

Conclusions

Neutron diffraction data has indicated that a sample of nominal starting composition, "$La_{9.5}Mn_{0.5}(GeO_4)_6O_{2.75}$", is actually better represented as $La_{9.18}Mn_{0.28}(GeO_4)_{5.8}(MnO_4)_{0.2}O_2$, illustrating the fact that Mn is an ambi-site dopant, substituting on both the La and Ge site in this phase. It also suggests that cation vacancies are preferable in the apatite structure to interstitial oxide ions in this doped system. The space group was determined to be $P6_3/m$, although high thermal displacement parameters were observed indicative of static disorder, modelled by split sites. The work therefore suggests that in this, and other apatite systems, there is likely to be significant local regions of lower symmetry.

Acknowledgements

We would like to thank ISIS, RAL for the provision of neutron diffraction beam time.

References

1. S. Nakayama, H. Aono, Y. Sadaoka, Chem. Lett. (1995) 431.

2. S. Nakayama, M. Sakamoto, M. Higuchi, K. Kodaira; J. Mater. Sci. Lett. 19 (2000) 91.

3. S. Nakayama, M. Higuchi; J. Mater. Sci. Lett. 20 (2001) 913.

4. H. Arikawa, H. Nishiguchi, T. Ishihara, Y. Takita, Solid State Ionics 136-137 (2000) 31.

5. J.E.H. Sansom, D. Richings, P.R. Slater, Solid State Ionics 139 (2001) 205.

6. L. Leon-Reina, M.C. Martin-Sedeno, E.R. Losilla, A. Cabeza, M. Martinez-Lara, S. Bruque, F.M.B. Marques, D.V. Sheptyakov, M.A.G. Aranda; Chem. Mater. 15 (2003) 2099.

7. L. Leon-Reina, E.R. Losilla, M. Martinez-Lara, S. Bruque, M.A.G. Aranda; J. Mater. Chem. 14 (2004) 1142.

8. J.R. Tolchard, M.S. Islam, P.R. Slater; J. Mater. Chem. 13 (2003) 1956.

9. H. Yoshioka and S. Tanase; Solid State Ionics 176 (2005) 2395.

10. E.J. Abram, C.A. Kirk, D.C. Sinclair, A.R. West; Solid State Ionics 176 (2005) 1941.

11. V.V. Kharton, A.L. Shaula, M.V. Patrakeev, J.C. Waerenborgh, D.P. Rojas, N.P. Vyshatko, E.V. Tsipis, A.A. Yaremchenko, F.M.B. Marques; J. Electrochem. Soc. 151 (2004) A1236.

12. J.E.H. Sansom, J.R. Tolchard, D. Apperley, M.S. Islam, P.R. Slater; J. Mater. Chem. 16 (2006) 1410.

13. L. Leon-Reina, J.M. Porras-Vasquez, E.R. Losilla, M.A.G. Aranda; J. Solid State Chem. 180 (2007) 1250.

14. E. Kendrick, J.R.Tolchard, J.E.H. Sansom, M.S. Islam, P.R. Slater; Faraday Discussions 134 (2007) 181.

15. E. Rodriguez-Reyna, A.F. Fuentes, M. Maczka, J. Hanuza, K. Boulahya, U. Amador; Solid State Sci. 8 (2006) 168.

16. S. Celerier, C. Laberty-Robert, J.W. Long, K.A. Pettigrew, R.M. Stroud, D.R. Rolison, F. Ansart, P. Stevens, Adv. Mater., 18 (2006**)** 615.

17. S. S. Pramana, W.T. Klooster and T. J. White; Acta Cryst. B 63 (2007) 597.

18. A. Chesnaud, C. Bogicevic, F. Karolak, C. Estournes, G. Dezaneau; Chem. Commun. (2007) 1550.

19. J.R.Tolchard, P.R. Slater, J. Phys. Chem. Solids 69 (2008) 2433.

20. J.R.Tolchard, J.E.H. Sansom, M.S. Islam, P.R. Slater; Dalton Trans. 7 (2005) 1273.

21. Y.V. Pivak, V.V. Kharton, A.A. Yaremchenko, S.O. Yakovlev, A.V. Kovalevsky, J.R. Frade, F.M.B. Marques, J. Euro Ceram Soc 27 (2007) 2445.

22. E. Kendrick, M.S. Islam, P.R. Slater; J. Mater. Chem. 17 (2007) 3104.

23. E. Kendrick, M.S.Islam, P.R. Slater; Chem. Commun (2008) 715.

24. J. R. Tolchard, P. R. Slater and M. S. Islam; Adv. Funct. Mater. 17 (2007) 2564.

25. Y.V. Pivak, V.V. Kharton, A.A. Yaremchenko, S.O. Yakovlev, A.V. Kovalevsky, J.R. Frade, F.M.B. Marques; J. Euro. Ceram. Soc. 27 (2007) 2445.

26. A. Orera, E. Kendrick, D. C. Apperley, V.M. Orera, P.R. Slater; Dalton Trans. (2008) 5296.

27. A. Jones, P.R. Slater, M.S. Islam; Chem Mater 20 (2008) 5055.

28. J.E.H. Sansom, P.R. Slater; Solid State Ionics 167 (2004) 23.

29. H. Yoshioka; J. Amer. Ceram. Soc. 90 (2007) 3099.

30. E. Kendrick, P.R. Slater; Mater. Res. Bull. 43 (2008) 2509.

31. E. Kendrick, P.R. Slater; Solid State Ionics 179 (2008) 981.

32. P.J. Panteix, I. Julien, P. Abelard, D. Bernache-Assolant; Ceram. Int. 34 (2008) 1579.

33. T. Iwata, K. Fukuda, E. Bechade, O. Masson, I. Julien, E. Champion, P. Thomas; Solid State Ionics 178 (2008) 1523.

34. R. Ali, M. Yashima, Y. Matsushita, H. Yoshioka, K. Okoyama, F. Izumi; Chem. Mater. 20 (2008) 5203.

35. S.S. Pramana, W.T. Klooster, T.J. White; J. Solid State Chem. 181 (2008) 1717.

36. E. Kendrick, D. Headspith, A. Orera, D.C. Apperley, R.I. Smith, M.G. Francesconi, P.R. Slater; J. Mater. Chem. 19 (2009) 749.

37. J.E.H. Sansom, E. Kendrick, A. Scullard, C. Olsen, M.S. Islam, P.A. Sermon; Proc 7th Euro SOFC Forum B051 (2006) 1.

38. A.C. Larson, R.B. Von Dreele. *Los Alamos National Laboratory, Report*. No LA-UR-86-748, 1987.

39. J. Ito; Am. Mineral. 53 (1968) 890.

40. E. Kluver, H. Müller-Buschbaum; Z. Naturforsch Teil B50 (1995) 61.

41. D.A. Grisafe, F.A. Hummel; J. Solid State Chem. 2 (1970) 160.

42. R. Klement, H. Haselbeck; Z. Anorg. Allgem. Chem. 336 (1965) 113.

Table 1. Refined structural parameters for $La_{9.18}Mn_{0.28}(GeO_4)_{5.8}(MnO_4)_{0.2}O_2$

Atom	Site	x	y	z	$100xU_{iso}$	Fractional occupancy
La1/Mn1	4f	1/3	2/3	0.0023(3)	1.32(6)	0.795/0.07
La2	6h	0.2420(1)	0.0112(2)	1/4	0.91(3)	1.0
Ge/Mn2	6h	0.3746(2)	0.4014(2)	1/4	0.57(3)	0.967/0.033
O1	6h	0.4738(2)	0.6039(2)	1/4	2.63*	1.0
O2	6h	0.4894(2)	0.3161(2)	1/4	2.42*	1.0
O3a	12i	0.231(1)	0.279(1)	0.092(1)	2.08*	0.260(8)
O3b	12i	0.2542(4)	0.3563(6)	0.0567(4)	2.08*	0.740(8)
O4	4e	0	0	0.2099(8)	2.0(1)	0.5

*Anisotropic thermal displacement parameters

	U11	U22	U33	U12	U13	U23
O1	0.9(1)	0.6(1)	6.1(2)	0.08(10)	0	0
O2	2.0(1)	4.0(2)	2.1(1)	2.8(1)	0	0
O3a	2.4(2)	3.3(3)	0.6(1)	1.7(2)	-0.15(10)	-0.5(2)
O3b	2.4(2)	3.3(3)	0.6(1)	1.7(2)	-0.15(10)	-0.5(2)

$P6_3/m$, a=b= 9.88923(4), c=7.24127(5) Å

Bank1: R_{wp} = 0.0351; Bank2: R_{wp} = 0.0326; Total R_{wp}= 0.0335

Bank1: Rp= 0.0318; Bank2: R_p= 0.0284; Total R_p= 0.0306

χ^2=3.887

Table 2. Selected bond distances for $La_{9.18}Mn_{0.28}(GeO_4)_{5.8}(MnO_4)_{0.2}O_2$

Bond	Bond distance/Å	Bond	Bond distance/Å
La1-O1 [x3]	2.529(2)	La2-O4 [x2]	2.358(1)
La1-O2 [x3]	2.478(2)	La2-O3b [x2]	2.450(2)
La1-O3b [x3]	2.791(5)	La2-O3b [x2]	2.670(4)
La2-O1	2.531(2)	Ge-O1	1.734(2)
La2-O2	2.775(3)	Ge-O2	1.720(2)
La2-O3a [x2]	2.935(1)	Ge-O3a [x2]	1.752(9)
La2-O3a [x2]	2.476(9)	Ge-O3b [x2]	1.745(3)
La2-O3a [x2]	2.504(7)		

Figure Legends

Figure 1. The apatite structure adopted by $Ln_{9.33+x}(Si/GeO_4)_6O_{2+3x/2}$ (Ln=rare earth) ionic conductors ($Ln_{3.33+x}(Si/GeO_4)_6$ framework represent by the tetrahedra and trigonal metaprisms; large sphere = Ln, small sphere = O).

Figure 2. Observed, calculated and difference neutron diffraction profiles for $La_{9.18}Mn_{0.28}(GeO_4)_{5.8}(MnO_4)_{0.2}O_2$

Figure 3. Conductivity data for $La_{9.18}Mn_{0.28}(GeO_4)_{5.8}(MnO_4)_{0.2}O_2$

Fig 1.

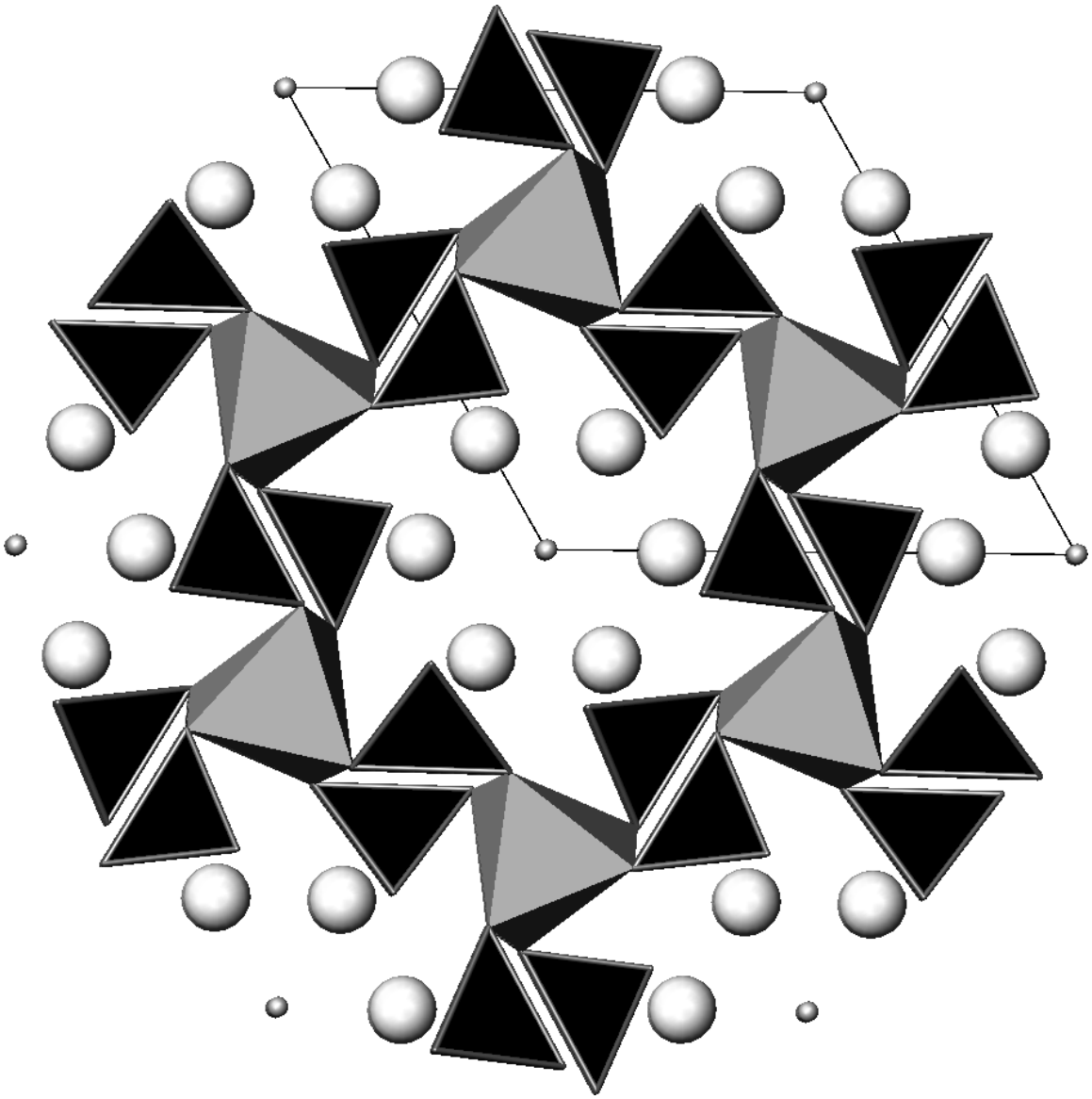

Fig 2.

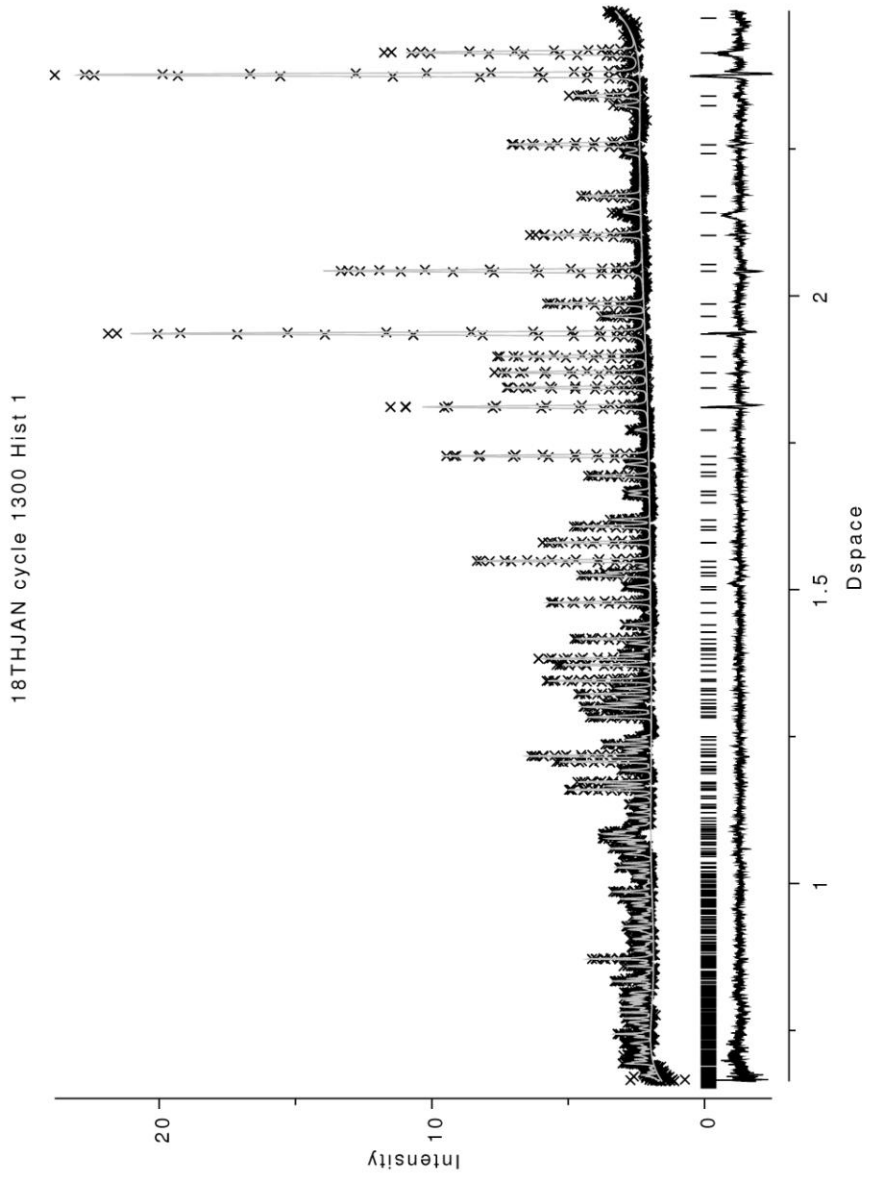

Fig 3.